Journal of Coordination Chemistry

ISSN: 0095-8972 (Print) 1029-0389 (Online) Journal homepage: http://www.tandfonline.com/loi/gcoo20

Highly soluble tetra lauryl alcohol substituted phthalocyanines; synthesis, electrochemistry, spectroelectrochemistry

Ahmet T. Bilgiçli, M. Nilüfer Yaraşir, Mehmet Kandaz & Atif Koca

To cite this article: Ahmet T. Bilgiçli, M. Nilüfer Yaraşir, Mehmet Kandaz & Atif Koca (2015) Highly soluble tetra lauryl alcohol substituted phthalocyanines; synthesis, electrochemistry, spectroelectrochemistry, Journal of Coordination Chemistry, 68:2, 350-366, DOI: 10.1080/00958972.2014.986472

To link to this article: http://dx.doi.org/10.1080/00958972.2014.986472

Accepted author version posted online: 17 Nov 2014.

Journal of Coordination Chemistry, 2015
Vol. 68, No. 2, 350–366, http://dx.doi.org/10.1080/00958972.2014.986472

Highly soluble tetra lauryl alcohol substituted phthalocyanines; synthesis, electrochemistry, spectroelectrochemistry

AHMET T. BILGIÇLI†, M. NILÜFER YARAŞIR†, MEHMET KANDAZ*† and ATIF KOCA‡

†Department of Chemistry, Sakarya University, Esentepe, Turkey
‡Faculty of Engineering, Department of Chemical Engineering, Marmara University, Istanbul, Turkey

(*Received 22 July 2014; accepted 17 October 2014*)

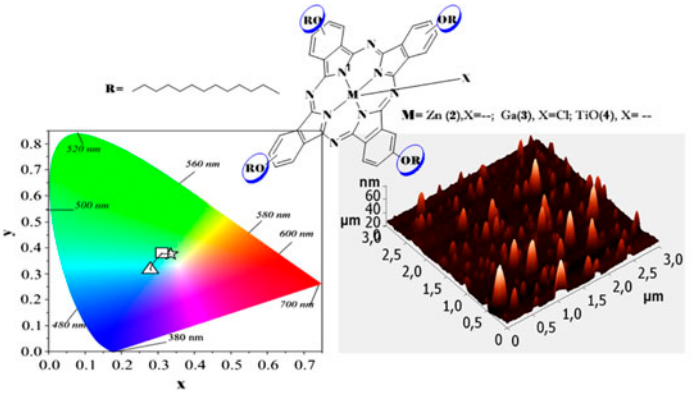

The tetra peripherally *β*-substituted 2(3),9(10),16(17),23(24)-tetrakis undecyloxy phthalocyanine derivatives, M{Pc[O-$(CH_2)_{11}CH_3)]_4$} Pc: Phthalocyanine, [M: Zn(II)(**2**), Ga(III)(**3**), and Ti(IV)(**4**)], have been synthesized and characterized using FT-IR, ^{1}H, and ^{13}CNMR, MS (MALDI-TOF), UV–vis, atomic force microscopy, electro and spectroelectro chemical and elemental analysis. The new synthesized complexes are soluble in both polar solvents and nonpolar solvents, such as THF, DMF, $CHCl_3$, CH_2Cl_2, benzene, and even hexane. Electrochemical and spectroelectrochemical measurements give common metal-based and/or Pc ring-based redox processes which support the proposed structures of the complexes. While titanium phthalocyanine exhibits metal- and Pc ring-based reduction and/or oxidation couples, gallium and zinc phthalocyanines give only Pc ring-based electron transfer processes.

Keywords: Phthalocyanine; Zinc; Gallium and Titanium; Synthesis; Spectroelectrochemistry; Electrocolorimetry

*Corresponding author. Email: mkandaz@sakarya.edu.tr

1. Introduction

Efforts in the development of new types of highly soluble metallophthalocyanine (MPcs) complexes have been increasing due to their applications in chemical sensors [1], liquid crystals [2, 3], photodynamic therapy [4, 5], data storage [6], and non-linear optics [7].

The high-tech capabilities of Pcs materials depend not only on the molecular composition including the metal center and the number, position, and nature of the substituents, but also on the molecular architecture [8]. For example, the molecular arrangement (balance between hydrophobic and hydrophilic properties) in the core and on the periphery is a determining factor controlling many of the physical properties of the macrocycles including the electrical photoconductivity, magnetic susceptibility, and optical non-linearity [9]. By functionalizing the phthalocyanine ring with long aliphatic chains, the solubility increases and liquid crystalline compounds can be obtained. Phthalocyanines substituted with hydrophilic aliphatic alcohol, aliphatic thioalcohol, or polyaliphatic alcohol chains increase solubility in polar solvents, such as MeOH, EtOH, *i*-PrOH, THF, CH_3CN, and even in water [10–13]. Moreover, introduction of adequate functional/non-functional substituents on the periphery and non-peripheral positions of the phthalocyanine ring not only improves their solubility by causing substantial disruption of the strong interaction of the parent phthalocyanine rings but also increases their applications [14, 15]. For example, the PDT properties of the phthalocyanine dyes are strongly influenced by the presence and nature of the central metal ion and substituents. Also, the presence of electron-donating/electron-withdrawing substituents is a useful way of regulating the wavelength of the Q band to longer or short wavelengths [12–14]. Functional phthalocyanines are of particular chemical interest because of their tendency to aggregate in self-assemblies, optical and electrochemical responses to specific analytes, and capable of binding multiple metal ions for the development of new molecules/macrocycles [12, 15, 16]. In such systems, the metal in the central macrocyclic cavity and periphery can be chosen independently, thus giving physical properties not seen in the phthalocyanine or metal fragment alone [17].

In this article, a new ligand, 4-(undecyloxy)-phthalonitrile, and its tetrasubstituted metallophthalocyanines, $M\{Pc[O\text{-}(CH_2)_{11}CH_3)]_4\}$ [M = Zn(II), Ga(III), and Ti(IV)], are described. Also in this study, we have performed voltammetric and *in situ* spectroelectrochemical characterization of the newly synthesized MPc complexes.

2. Experimental

Chloroform ($CHCl_3$), tetrahydrofuran (THF), 4-nitrophthalonitrile, 1-dodecanol, tetrabutyl ammoniumtetrafluoroborate ($TBATBF_4$), $Zn(OAc)_2$, $GaCl_3$, and titanium(IV) butoxide ($Ti(OBu)_4$) were purchased from Merck and Alfa Aesar and used as received. All other reagents were obtained from Fluka, Aldrich and Alfa Aesar Chemical Co. and used without purification. The purity of the products was tested in each step by TLC (SiO_2, $CHCl_3$/MeOH, and THF/MeOH). FT-IR spectra were recorded on a Perkin–Elmer FT-IR spectrophotometer where samples were dispersed in KBr. Chromatography was performed with silica gel (Merck grade 60 and Sephadex) from Aldrich. Elemental analyses (C, H, and N) were performed at the Instrumental Analysis Laboratory of Marmara University. Time-resolved UV–vis spectra were recorded on an Agilent model 8453 diode array spectrophotometer. ^{1}HNMR and ^{13}CNMR spectra were recorded on a Bruker 300 spectrometer. Mass

spectra were acquired on a Voyager-DETM PRO MALDI-TOF mass spectrometer (Applied Biosystems, USA) equipped with a nitrogen UV laser operating at 337 nm. Spectra were recorded in reflectron mode with average of 50 shots. 2,5-Dihydroxybenzoic acid (DHB) (20 mg mL^{-1} in THF) matrix for **1**, **2**, **3**, and **4** was prepared. MALDI samples were prepared by mixing complex (2 mg mL^{-1} in THF) with the matrix solution (1 : 10 v/v) in a 0.5 mL Eppendorf® micro tube. Finally, 1 μL of this mixture was deposited on the sample plate, dried at room temperature, and then analyzed. Photo-irradiations were measured using a General Electric quartz line lamp (300 W). A 600 nm glass cut off filter (Schott) and a water filter were used to filter off ultraviolet and infrared radiations, respectively.

2.1. *Synthesis*

2.1.1. 4-(Undecyloxy) phthalonitrile (1). 1-Dodecanol (1.10 g) was dissolved in dry DMF (10 cm^3) and then finely ground anhydrous K_2CO_3 (~2.00) was added. To this was added dropwise 4-nitrophthalonitrile (1.00 g) in DMF (10 cm^3) at 40 °C in N_2 atmosphere. The reaction mixture was stirred efficiently and monitored by thin-layer chromatography (TLC) under inert atmosphere at 40–45 °C for 2 days. After the reaction mixture was cooled to room temperature, it was poured into ca. 300 cm^3 ice water. The creamy precipitate was filtered and washed with water until washing became neutral. The crude product was dissolved in $CHCl_3$ and washed with 5% $NaHCO_3$ to remove unreacted excess alcohol compounds. The creamy solution was then dried with anhydrous Na_2SO_4 and filtered. The solvent, $CHCl_3$, was removed under reduced pressure giving a creamy powder. It was chromatographed over silica gel column using a mixture of $CHCl_3$: MeOH (100/5) as eluent, giving a hydroscopic oily solid, 4-(undecyloxy) phthalonitrile (**1**). Yield: 1.30 g (75.11%). M.p.: oily at r.t. °C, IR (KBr) ν/cm^{-1}: 3103, 3082, 3039 (w, Ar–H), 2918, 2850 (Aliph–CH_2), 2229(st), 1602 (C=N), 1562 (C=C), 1473, 1396, 1309, 1294, 1282, 1249, 1093, 1020, 1001, 968, 914, 871, 833, 715; ^{1}H NMR ([D_6]-DMSO) δ: 8.02 (dd, 1H, meta to Ar–OR and CN, phenyl H5), 7.67 (d, isomer, 1H, ortho to Ar–OR, phenyl H4), 7.41 (d, 1H, Ar–H6), 4.11 (–*CH_2*–O), 3.30 (DMSO), 2.12 (2H, *CH_2*–CH_2O), 1.73–1.40 (4H,OCH_2*CH_2*$CH_2CH_2CH_2CH_2CH_2CH_2CH_2CH_2CH_3$), 1.20–1.30 (16H, *$CH_2CH_2CH_2CH_2CH_2CH_2CH_2CH_2$*$CH_3$), 0.82 (3H, –$CH_2$*$CH_3$*); ^{13}C NMR ([300 MHz, δ, D6]-DMSO): 162.73 (C3, *CH_2*–O), 136.43(Ar–C5), 134.92 (Ar–C6), 120.69 (Ar–C4), 116.956 (Ar–C2), 116.95 (C1, Ar–CN), 115.43(Ar–CN), 109.39 (Ar–CN), 69.69 (*CH_2*O), 40.165 (DMSO), 33.23 (*$CH_2CH_2CH_3$*), 29.72 –OCH_2CH_2(*CH_2*)$_8CH_2CH_3$ 22.66(*CH_2CH_3*), 14.63 (CH_3) ppm. Anal. Calcd for $C_{20}H_{28}N_2O$ (%): C, 76.88; H, 9.03; N, 8.97. Found (%): C, 76.56; H, 9.45; N, 9.17. MALDI-MS: 313,5 $[M + H]^+$.

2.1.2. [Zn] 2(3), 9(10), 16(17), 23(24)-tetrakis undecyloxy phthalocyanine (2). A mixture of **1** (0.25 g) and 1,8-diazabicycloundec-7-ene (DBU) (0.05 cm^3) in a sealed tube was dissolved and heated with efficient stirring at 160 °C for 0.5 h under N_2 in *n*-hexanol (~1.0 cm^3) and then anhydrous Zn(acac)$_2$ (0.04 g, 0.24 mM) was added. After heating and stirring for 6 h, the deep green–blue product was cooled to RT, and solid was washed successively with hot MeOH and CH_3CN, copious mixture of *i*-PrOH and water, cold CH_3CN to remove impurities until the filtrate was clear. The green–blue product was isolated by silica gel column chromatography with $CHCl_3$–MeOH (20/1 v/v) as eluent. Complex **2** was purified again with a second column chromatography over Sephadex (5% $CH_3OH/CHCl_3$, eluent) and then dried *in vacuum*. Complex **2** is moderately soluble in $CHCl_3$, CH_2Cl_2,

THF, DMF, DMAA, and pyridine. Yield: 0.021 g (35%). M.p.: >200 °C. Anal. Calcd for $C_{80}H_{112}N_8O_4Zn$ (1313 g M^{-1}): C, 73.06; H, 8.58; N, 8.52. Found: C, 73.56; H, 8.51; N, 9.02. IR (KBr) ν/cm^{-1}: 3041 (Ar–H), 2924, 2852, 1643, 1604, 1582, 1487, 1463, 1386, 1361, 1336, 1278, 1228, 1192, 1118, 1085, 1047, 945, 873, 825, 746. ^{1}H NMR ([D_6]-DMSO) δ: 8.07 (d, br 1H, meta to Ar–OR and CN, phenyl H5), 7.84 (d, br, isomer, 1H, ortho to Ar–OR, phenyl H4), 7.73 (d, br, 1H, ortho to CN, Ar–H6), 4.08 (–*CH_2*–O), 3.30 (DMSO), 2.15 (8H, CH_2–*CH_2*O), 1.75–1.45 (16H, OCH_2*CH_2CH_2* $CH_2CH_2CH_2CH_2CH_2CH_2CH_2$ CH_2CH_2), 1.35–1.28 (16H,$OCH_2CH_2CH_2$*$CH_2CH_2CH_2CH_2$* *$CH_2CH_2CH_2CH_2$*CH_3), 0.86 (12H, –$OCH_2CH_2CH_2CH_2CH_2CH_2$ $CH_2CH_2CH_2$ CH_2CH_2 *CH_3*). UV/Vis (THF, λ_{max} nm^{-1}: 679 (Q), 611(*n*–π*, sh), 350 (B); MS (MALDI-TOF, dihydroxybenzoic acid (DHBA as matrix): *m/z*: 1314 $[M + H]^+$.

2.1.3. [Ga] 2(3), 9(10), 16(17), 23(24)-tetrakis undecyloxy phthalocyanine (3). Compound **1** (0.25 g) and anhydrous $GaCl_3$ (0.015 g) in *n*-hexanol (~1.00 cm^3) were heated to reflux in a sealed tube under N_2 for 6 h. The color of the mixture turned green–blue during reflux. After heating was continued for an additional 2 h, the green–blue product was cooled to room temperature after which the mixture was washed with MeOH. The crude product was washed several times successively with first *i*-PrOH and then cold CH_3CN to remove impurities. Finally, the product was further purified by silica gel chromatography with $CHCl_3$/MeOH (20 : 1 v/v). This product is soluble in $CHCl_3$, CH_2Cl_2, THF, DMF, and pyridine. Yield: 0.013 g (21%). M.p.: >200 °C. Anal. Calcd for $C_{80}H_{112}N_8O_4GaCl$ (1353 g M^{-1}): C, 70.91; H, 8.33; N, 8.27. Found: C, 72.7; H, 8.68; N, 8.42. FT-IR (KBr) ν cm^{-1}: 3042 (Ar–H), 2922, 2850 (Aliph–H), 1714, 1606, 1506, 1487, 1463, 1408, 1388, 1342, 1321, 1274, 1230, 1116, 1089, 1053, 1010, 950, 871, 823, 746. ^{1}H NMR ([D_6]-DMSO) δ: 8.02 (d, br 4H, meta to Ar–OR and CN, phenyl H5), 7.80 (d, br, isomer, 4H, ortho to Ar–OR, phenyl H4), 7.73 (d, br, 4H, ortho to CN, Ar–H6), 4.12 (–*CH_2*–O), 3.30 (DMSO), 2.05 (8H, CH_2–*CH_2*O), 1.70–1.42 (16H, OCH_2*CH_2CH_2*CH_2 CH_2CH_2 $CH_2CH_2CH_2CH_2$ CH_2CH_2), 1.35–1.28 (16H, OCH_2CH_2 CH_2*$CH_2CH_2CH_2CH_2CH_2$* *$CH_2CH_2CH_2$*CH_3), 0.88 (12H, -$OCH_2CH_2CH_2CH_2CH_2$ CH_2CH_2 $CH_2CH_2CH_2CH_2$*CH_3*). UV–vis (THF), λ_{max} nm^{-1}: 695 (Q), 631 (*n*–π*), 344(B); MS (MALDI-TOF, dihydroxybenzoic acid (DHBA as matrix): *m/z* (%): 1354.5 $[M + H]^+$.

2.1.4. [Ti] 2(3), 9(10), 16(17), 23(24)-tetrakis undecyloxy phthalocyanine (4). Compound **1** (0.25 g), anhydrous $Ti(OBu)_4$ (0.03 g), and DBU (0.05 cm^3) in *n*-hexanol (~1.00 cm^3) were heated to reflux in a sealed tube under N_2 for 6 h. After cooling to room temperature and washing with *i*-PrOH it was filtered. The dark green–blue crude product formed during the reaction was treated with *i*-PrOH several times and filtered off. It was then successively washed with MeOH and CH_3CN, and dried. Further purification by column chromatography with silica gel ($CHCl_3$/MeOH as an eluent, 20/1 v/v) and dried in vacuo. This phthalocyanine (**4**) is soluble in $CHCl_3$, CH_2Cl_2, THF, DMF, and pyridine. Yield: 0.018 g (30%). M.p.: >200 °C. Anal. Calcd for $C_{80}H_{112}N_8O_5Ti$ (1313 g M^{-1}): C, 73.14; H, 8.59; N, 8.53. Found: C, 74.01; H, 8.65; N, 8.89. FT-IR (KBr) ν/cm^{-1}: 3028, 2922, 2852, 1714, 1604, 1556, 1487, 1463, 1386, 1338, 1276, 1230, 1118, 1070, 1024, 966, 871, 823, 748. ^{1}H NMR ([D_6]-DMSO) δ: 8.00 (d, br 4H, meta to Ar–OR and CN, phenyl H5), 7.80 (d, br, isomer, 4H, ortho to Ar–OR, phenyl H4), 7.73 (d, br, 4H, ortho to CN, Ar–H6), 4.06 (–*CH_2*–O), 3.30 (DMSO), 2.00 (8H, CH_2–*CH_2*O), 1.70–1.42 (16H,

$OCH_2CH_2CH_2CH_2$ $CH_2CH_2CH_2CH_2$ CH_2CH_2 CH_2CH_2), 1.35–1.28 (16H, $OCH_2CH_2CH_2$ $CH_2CH_2CH_2CH_2CH_2CH_2CH_2CH_2CH_3$), 0.86 (12H, $-OCH_2CH_2$ $CH_2CH_2CH_2CH_2CH_2$ $CH_2CH_2CH_2CH_2CH_3$). UV/Vis (THF, λ_{max} nm^{-1}: 700(Q), 629 (n–π*), 347(B); MS (MALDI-TOF, dihydroxybenzoic acid (DHBA as matrix): *m/z*: 1314 $[M + H]^+$.

2.2. *Electrochemical* in situ *spectroelectrochemical and* in situ *electrocolorimetric measurements*

Cyclic voltammetry (CV) and square wave voltammetry (SWV) measurements were carried out with a Gamry Reference 600 potentiostat/galvanostat controlled by an external PC and utilizing a three-electrode configuration at 25 °C. The working electrode was a Pt disk with a surface area of 0.071 cm^2. A Pt wire served as the counter electrode. Saturated calomel electrode (SCE) was employed as the reference electrode and separated from the bulk of the solution by a double bridge. Electrochemical grade tetrabutylammonium perchlorate (TBAP) in extra pure dichloromethane (DCM) was employed as the supporting electrolyte at a concentration of 0.10 M dm^{-3}.

UV–vis absorption spectra and chromaticity diagrams were measured by an Ocean Optics QE65000 diode array spectrophotometer. *In situ* spectroelectrochemical measurements were carried out by utilizing a three-electrode configuration of a quartz thin-layer spectroelectrochemical cell at 25 °C. The working electrode was a Pt gauze semitransparent electrode. Pt wire counter electrode separated by a glass bridge and a SCE reference electrode separated from the bulk of the solution by a double bridge were used. *In situ* electro-colorimetric measurements, under potentiostatic control, were obtained using an Ocean Optics QE65000 diode array spectrophotometer at color measurement emission mode by utilizing a three-electrode configuration of the thin-layer quartz spectroelectrochemical cell. The standard illuminant A with 2 degree observer at constant temperature in a light booth designed to exclude external light was used. CIE standard illuminant A is intended to represent typical, domestic, tungsten-filament lighting. Its relative spectral power distribution is that of a Planckian radiator at a temperature of approximately 2856 K. Due to the nature of the distribution of cones in the eye, the tristimulus values depend on the observer's field of view. To eliminate this variable, the CIE defined the standard (colorimetric) observer. Originally this was taken to be the chromatic response of the average human viewing through a 2°. Thus, the CIE 1931 standard observer is also known as the CIE 1931 2° standard observer. Prior to each set of measurements, background color coordinates (x, y, and z values) were taken at open-circuit using the electrolyte solution without the complexes under study. During the measurements, readings were taken as a function of time under kinetic control; however, only the color coordinates at the beginning and end of each redox process were reported.

2.3. *Photodegradation quantum yields*

Photodegradation quantum yield (Φ_d) determinations were carried out using the experimental setup described [18–20]. Photodegradation quantum yields were determined using formula 1,

$$\Phi_d = \frac{(C_0 - C_t) \cdot V \cdot N_A}{I_{abs} \cdot S \cdot t} \quad (1)$$

where C_0 and C_t are the sample concentrations before and after irradiation, respectively, V is the reaction volume, N_A is the Avogadro's constant, S is the irradiated cell area, and t is the irradiation time. I_{abs} is the overlap integral of the radiation source light intensity and the absorption of the samples. A light intensity of 2.50×10^{16} photons s^{-1} cm^{-2} was employed for Φ_d determinations.

3. Results and discussion

Although phthalocyanine complexes have low solubility in most organic solvents, phthalocyanines bearing long aliphatic substituents on the Pc core increase the solubility. All synthesized phthalocyanine derivatives (**2–4**) have excellent solubility in most organic solvents. Ligand, 4-(undecyloxy) phthalonitrile (**1**), and its Zn(II), Ga(III), Ti(IV) phthalocyanines (**2**, **3**, and **4**) were prepared. Pcs (**2–4**) were accomplished by heating a pulverized mixture of 4-(undecyloxy) phthalonitrile with anhydrous $Zn(O_2CMe)_2$, $GaCl_3$, and $Ti(OBu)_4$ salts or without metal salt at ca. 150–160 °C under N_2 atmosphere in the presence of 1,8-diazabicyclo [5.4.0] undec-7-ene (DBU) for 6 h (scheme 1). The yields of these reactions were rather low (35.60 for **2**, 21.33 for **3**, and 25.10% for **4**). The phthalocyanines (**2**, **3**, and **4**) were characterized by FT-IR, ^{1}HNMR, UV/Vis and MALDI-TOF MS spectroscopic methods, as well as by elemental analysis. All the analytical and spectral data are consistent with the predicted structures.

Cyclotetramerization of 4-(undecyloxy) phthalonitrile to the phthalocyanines (**2–4**) was confirmed by disappearance of the sharp –C≡N vibration at 2229 cm^{-1}. IR spectra of phthalocyanines (**2–4**) are very similar with the exception of small stretching shifts. The ^{1}H NMR spectra of **2**, **3**, and **4** are somewhat broader than the corresponding signals in the starting 4-(undecyloxy) phthalonitrile (**1**) derivative. This broadening is likely due to chemical exchange caused by aggregation–disaggregation equilibria, and the fact that the product obtained in these reactions is a mixture of positional isomers which are expected to show chemical shifts that differ slightly from each other. The peripheral $–OCH_2$ proton at 4.00–4.14 ppm in **1** and **2**, and **3** and **4** was easily identified in the ^{1}H NMR spectrum with a broad chemical shift especially in the case of **2**, **3**, and **4** [11, 21, 22]. The other resonances related to different CH_2, CH_3, and Ar–H protons in the ^{1}H NMR spectra of **2**, **3**, and **4** are very similar to those of the 4-(undecyloxy) phthalonitrile.

UV–vis spectra of the phthalocyanine complexes exhibit characteristic Q and B bands, one in the visible region at ca. 600–750 nm (Q band) attributed to the π–π* transition from HOMO to the LUMO of the Pc^{2-} ring, and the other in the UV region at ca. 300–400 nm (B-band) arising from the deeper π–π* transitions [10]. The ground state electronic spectra of the compounds showed characteristic absorptions in the Q band region at 679 nm for **2**, 695 nm for **3**, and 700 for **4** in THF. B band absorptions of the metallophthalocyanines **2–4** were observed at 350, 344, and 347, respectively (figure 1).

The aggregation behaviors of **2**, **3**, and **4** were also investigated at different concentrations in THF to determine aggregation that depends on concentration (figure 2 as an example for (**2**). As shown in the figure, the Q band increases in intensity with increasing concentration of **2** and no new band was observed due to the aggregated species [18, 19]. Beer–Lambert Law was obeyed for **2**, **3**, and **4** in the concentration range 6.95–25 $\times 10^{-6}$ M dm^{-3}.

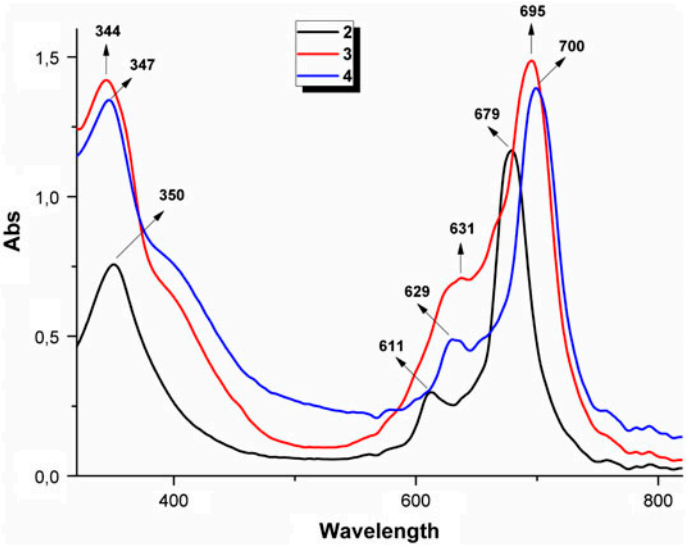

Figure 1. UV–vis spectra of **2**, **3** and **4** in THF.

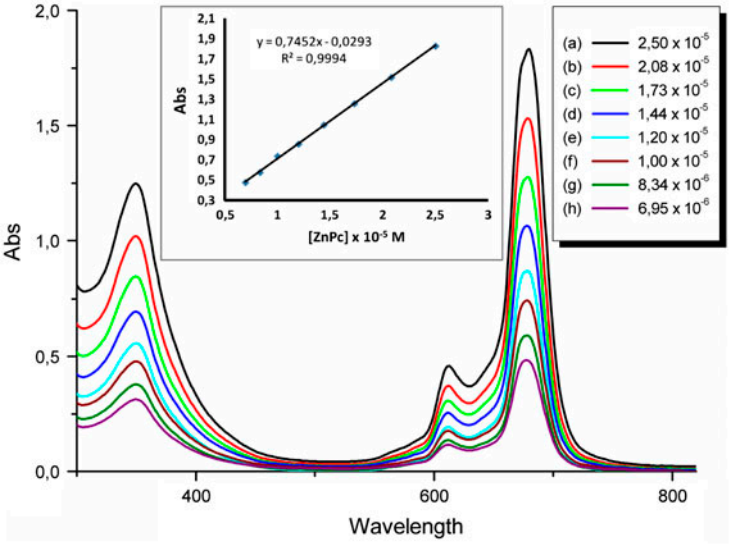

Figure 2. Absorption spectra of ZnPc (**2**) in THF at different concentrations (inset: plot of absorbance *vs*. concentration at 697 nm).

The bathochromic shift of the Q band due to the solvent for **2** increased in the following order: THF < DMF < $CHCl_3$ [figure 3(a)]. The electronic absorption spectra of **2** in these solvents were analyzed using the method described originally by Bayliss [23]. Figure 3(b) displays a plot of the Q band frequency *versus* the function $(n^{2-1})/(2n^2 + 1)$, where n is the refractive index of the solvent. The positions of the Q bands in these solvents show almost

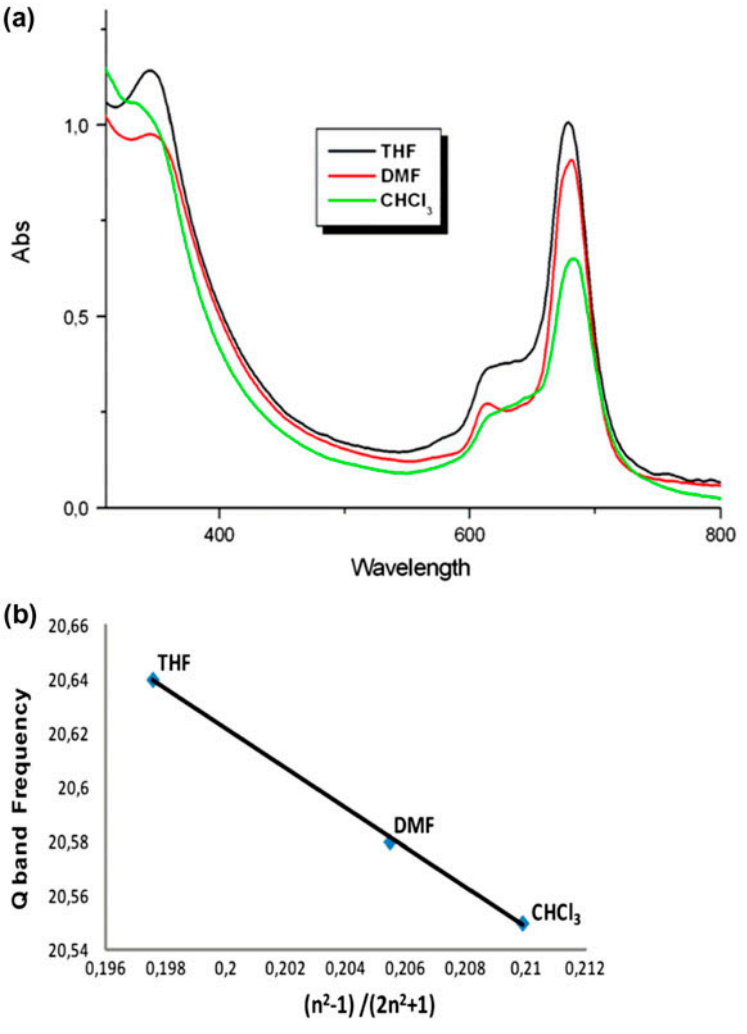

Figure 3. Absorption spectra of **2** in different solvents (1.4×10^{-5} M) (a) and plot of the Q band frequency of **2** against $(n^{2-1})/(2n^2 + 1)$ (b), where n is the refractive index of the solvent.

a linear dependence on this function. This linearity suggests that shifts are mainly due to solvation and not to a ligation effect [24].

The degradations of the phthalocyanine molecules were performed. The determination of the degradation of the molecules under irradiation is especially important for use as photocatalysts. The spectral changes obtained for all the studied phthalocyanine compounds (**2**, **3**, and **4**) in DMF during light irradiation are as shown in figure 4 (using complex **2** as an example). The collapse of the absorption spectra without any distortion of the shape confirms photodegradation not associated with phototransformation for **2**, **3**, and **4**. The photodegradation quantum yield (Φ_d) values for the complexes listed in n are of the order of 10^{-4}. Stable ZnPc molecules show values as low as 10^{-6}, and for unstable molecules,

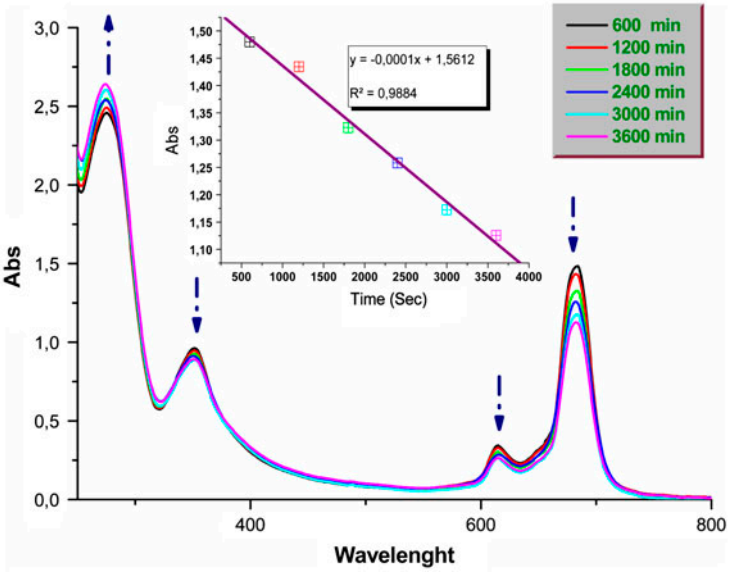

Figure 4. Absorption changes during the photodegradation studies of **2** in DMF showing the disappearance of the Q band at 10 min intervals (inset: plot of absorbance *vs.* time).

values of the order 10^{-3} have been reported [25]. Photodegradation quantum yields of **2**, **3**, and **4** have an average stability under applied light.

The morphology of thin film is important for electronic devices, and therefore, we examined the surface morphology of **2**, **3**, and **4**. Figure 5 shows 3-D AFM image of the **2**, **3**, and **4** phthalocyanine thin films (table 1).

3.1. *Voltammetric characterization*

Solution redox properties of ZnPc (**2**), GaPc (**3**), and TiOPc (**4**) were obtained in DCM/TBAP electrolyte system on a Pt working electrode. Table 2 lists the assignments of the redox couples and estimated electrochemical parameters including the half-wave peak potentials ($E_{1/2}$), ratio of the anodic to the cathodic peak currents ($I_{p,a}/I_{p,c}$), peak-to-peak potential separations (ΔE_p), and difference between the first oxidation and reduction processes ($\Delta E_{1/2}$). $\Delta E_{1/2}$ reflects the HOMO–LUMO gap for metal free Pcs, and it is related with the HOMO–LUMO gap in MPc species having redox inactive metal centers. Peak-to-peak separations, $E_{1/2}$ and $\Delta E_{1/2}$ values are in agreement with the reported data for redox processes of the metallophthalocyanine complexes [26–31].

Complexes **2** and **3** have both redox inactive metal centers and indicate very similar Pc ring-based electron transfer processes; thus, CV and SWV of **GaPc** (**2**) are given in figure 6 as representative of these complexes. Within the electrochemical window of DCM/TBAP, **3** has two one-electron oxidation and two one-electron reduction processes. For the first and second reduction couples, the anodic-to-cathodic peak separations (ΔE_p) changed from 90 to 210 mV with scan rates from 10 to 500 mV s^{-1}, indicating electrochemical irreversibility of these electron transfer processes. Irreversibility of these processes is illustrated by the shifting of the symmetry of the forward and reverse SWVs (figure 6) [32]. Unity of the

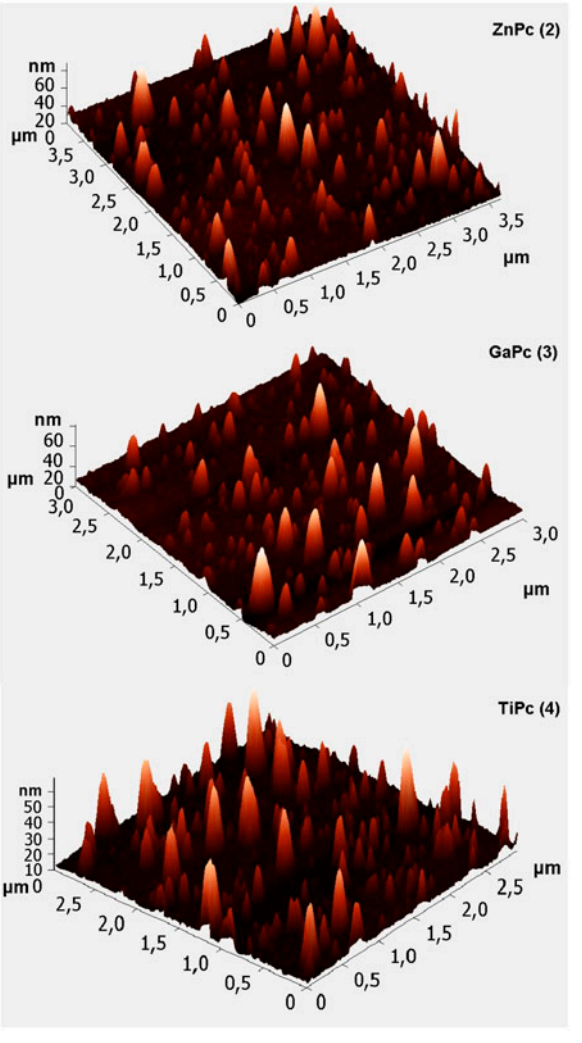

Figure 5. 3-D AFM image of ZnPc (**2**), GaPc (**3**) and TiPc (**4**).

Table 1. Photochemical properties of **2**, **3** and **4** in DMF.

Complex	Solvent	Φ_d (10^{-3})
2	DMF	0.3
3	DMF	0.2
4	DMF	0.2

I_{pa}/I_{pc} ratio with the scan rate and linear variation of the I_{pc} with square root of the scan rates indicated diffusion-controlled electron transfer mechanism of these processes. Oxidation processes are chemically and electrochemically irreversible completely, since they did not give cathodic couples during CV measurement. Observation of the cathodic couples of

Table 2. Voltammetric data of the complexes.

Complex		Ring oxidations		$Ti^{IV}O/Ti^{III}O$	$Ti^{III}O/Ti^{II}O$	Ring reductions		[d]$\Delta E_{1/2}$	Ref.
ZnPc	[a]$E_{1/2}$ *vs.* SCE	0.98[e]	0.71			−0.88	−1.33	1.59	
	[b]ΔE_p (mV)	–	105			120	155		Tw
	[c]I_{pa}/I_{pc}	–	0.77			0.89	0.84		
GaPc	[a]$E_{1/2}$ *vs.* SCE	1.40	0.83			−0.85	−1.20	1.68	
	[b]ΔE_p (mV)	–	–			110	158		Tw
	[c]I_{pa}/I_{pc}	–	–			0.92	0.90		
TiOPc	[a]$E_{1/2}$ *vs.* SCE	1.42	0.82 (1.08)	−0.64	−0.99	−1.45[e]		1.46	
	[b]ΔE_p (mV)	–	–	62	68	–			Tw
	[c]I_{pa}/I_{pc}	–	–	0.97	0.86	–			

[a]$E_{1/2} = (E_{pa} + E_{pc})/2$ at 0.100 Vs^{-1}.
[b]$\Delta E_p = |E_{pa} - E_{pc}|$ at 0.100 Vs^{-1}.
[c]I_{pa}/I_{pc} for reduction, I_{pc}/I_{pa} for oxidation processes at 0.100 Vs^{-1} scan rate.
[d]$\Delta E_{1/2} = \Delta E_{1/2}$ (first oxidation) $-\Delta E_{1/2}$ (first reduction) = HOMO–LUMO gap for metallophthalocyanines having electro-inactive metal center (metal to ligand (MLCT) or ligand to metal (LMCT) charge transfer gap for MPc having redox active metal center.
[e]The process is recorded with SWV.
Tw: This work.

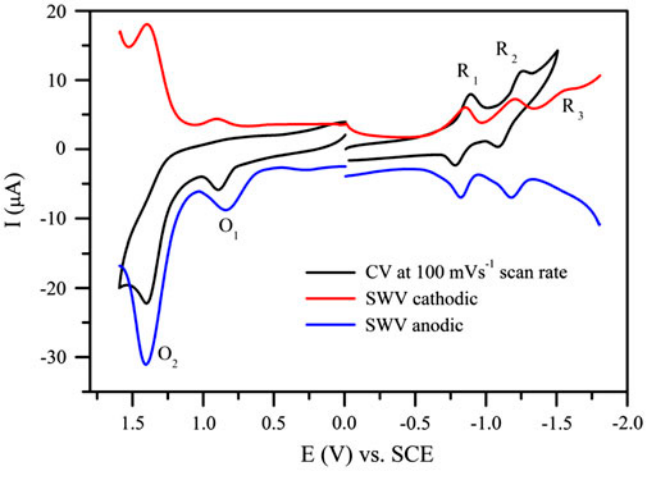

Figure 6. CVs and SWV of GaPc (5.0×10^{-4} M dm^{-3}) at 0.100 mV s^{-1} scan rate on Pt in DCM/TBAP (SWV parameters: pulse size = 100 mV; step size: 5 mV; frequency: 25 Hz).

the oxidation processes during SWV measurements indicates effects of the time scale of the voltammetric methods to the reversibility of these electron transfer processes (figure 6). Assignments of the redox couples are performed by spectroelectrochemical measurements given below.

Figure 7 shows CV SWVs of **TiPc** (**4**). Within the potential windows, two oxidation processes labeled as O_1 at 0.81 V and O_2 at 1.41 V and three reduction processes labeled as R_1 at −0.63 V, R_2 at −0.99 V, and R_3 at −1.45 V are observed. An unusual wave at 1.10 V is recorded at fast scan rates. We could not perform assignments of this wave due to decomposition of the complex under controlled potential during spectroelectrochemical measurement (given below). Unity of the $I_{p,a}/I_{p,c}$ ratios of the R_1 and R_2 couples at all scan rates indicate purely diffusion-controlled and chemically reversible behavior of the processes. ΔE_p values of these processes are in the electrochemical reversibility range. However, R_3 and oxidation

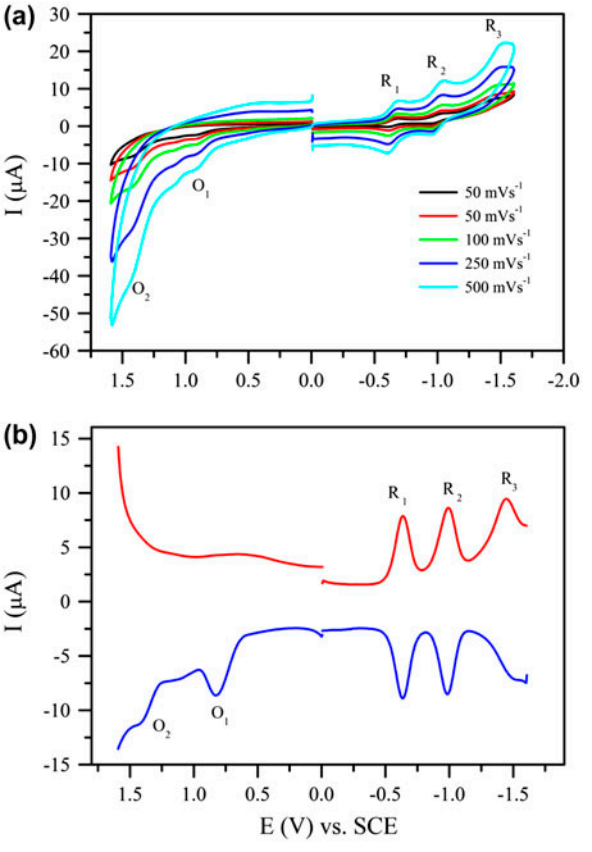

Figure 7. (a) CVs of **TiOPc** (5.0×10^{-4} M dm^{-3}) at various scan rates on Pt in DCM/TBAP. (b) SWV of **TiOPc**, SWV parameters: pulse size = 100 mV; step size: 5 mV; frequency: 25 Hz.

processes are not chemically reversible with respect to the $I_{p,a}/I_{p,c}$ ratio. Moreover, reversibility of the processes can be concluded with respect to symmetry and unity of the peak current ratios for the waves recorded during the forward and reverse SWV scans [figure 7(b)] [32].

3.2. In situ *spectroelectrochemical measurements*

Spectroelectrochemical studies were also employed to confirm the assignments in the CVs of MPcs. Figure 8 represents the *in situ* UV–vis spectral changes and *in situ* recorded chromaticity diagram of **GaPc** in DMSO/TBAP during potential applications at the potentials of the redox processes. There isn't any study illustrating the *in situ* spectroelectrochemical behavior of GaPcs in the literature; thus, this is the first article representing the *in situ* spectroelectrochemical changes of GaPc. Figure 8(a) illustrates the spectral changes during the first reduction process ($E_{app} = -1.00$ V). While the Q band at 698 nm decreases in intensity, two new bands enhance at 584 and 634 nm. The band at 634 nm increases and then shifts to higher energy side of the spectra. The band at 390 nm and the B band at

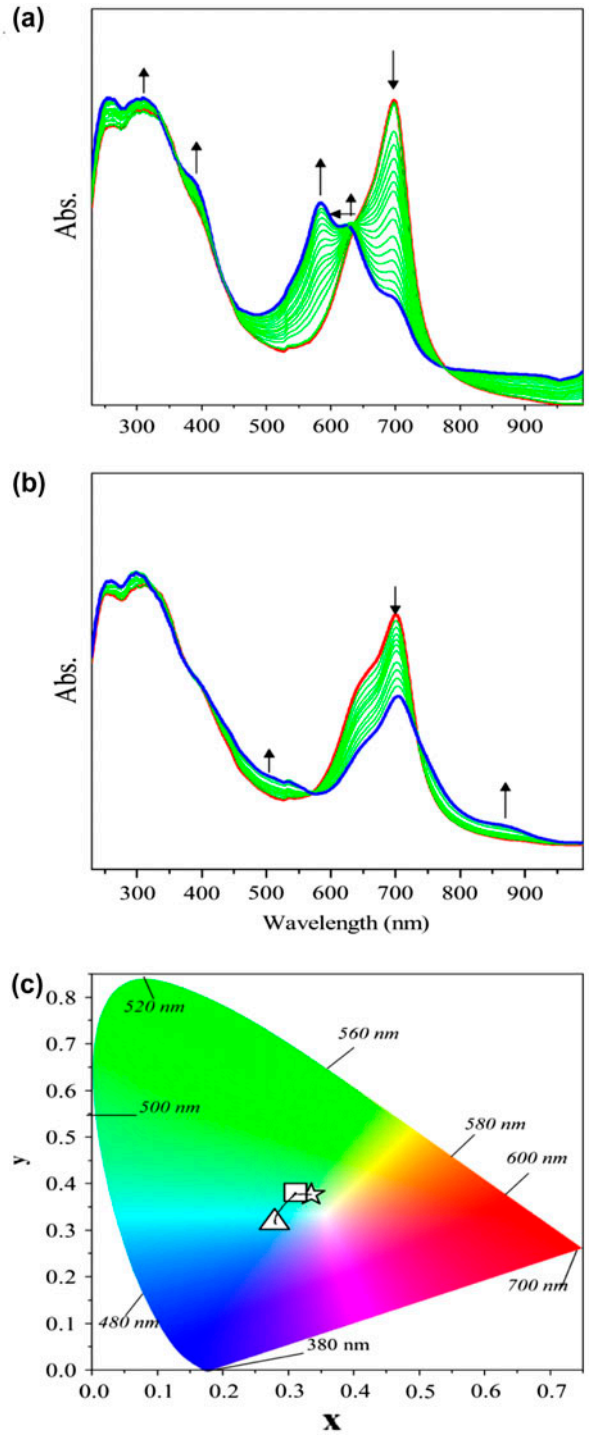

Figure 8. *In situ* UV–vis spectral changes of **GaPc** in DCM/TBAP electrolyte. (a) E_{app} = −1.00 V. (b) E_{app} = 1.00 V. (c) Chromaticity diagram of **GaPc** (each symbol represents the color of electro-generated species; □: [Cl–$Ga^{III}Pc^{-2}$], △: [Cl–$Ga^{III}Pc^{-3}]^{-1}$, ∇: $[Ga^{III}Pc^{-2}]^{+1}$.

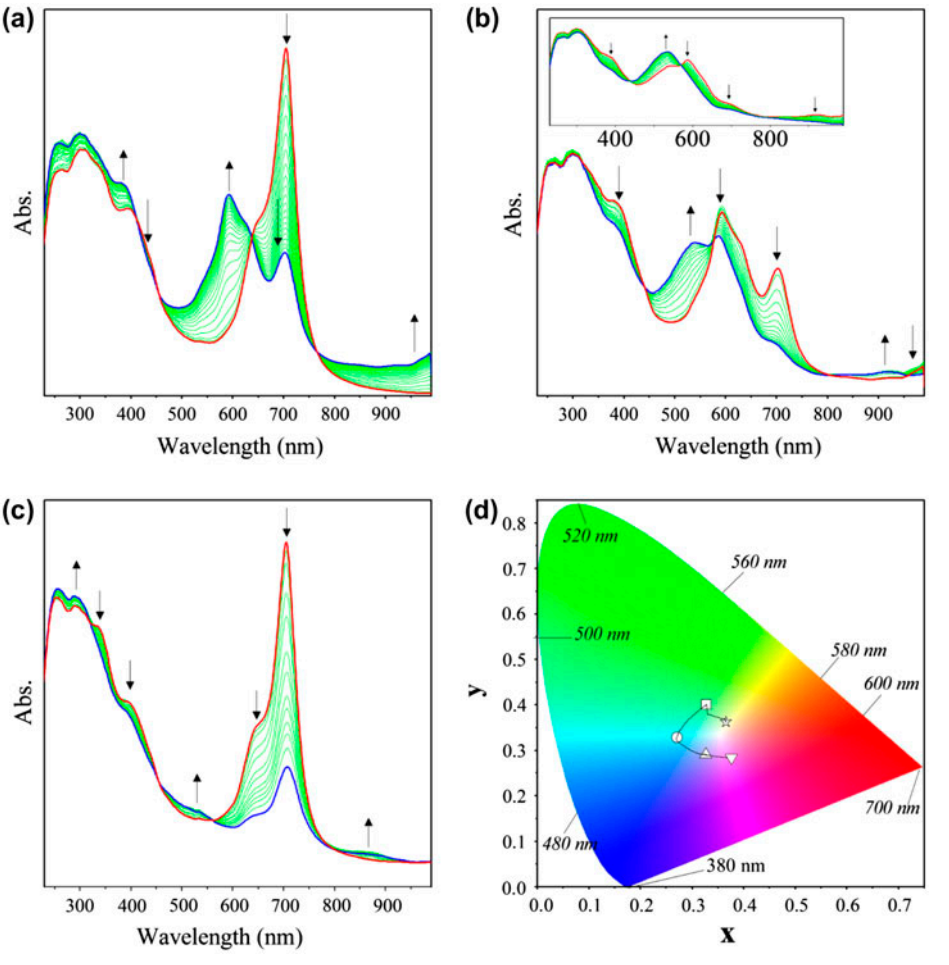

Figure 9. *In situ* UV–vis spectral changes of **TiOPc** in DCM/TBAP electrolyte. (a) $E_{app} = -0.75$ V. (b) $E_{app} = -1.25$ V (inset: $E_{app} = -1.75$ V). (c) $E_{app} = 1.00$ V. (d) Chromaticity diagram of **CoPc** (each symbol represents the color of electro-generated species; □: $[Ti^{IV}OPc^{-2}]$, ○: $[Ti^{III}OPc^{-2}]^{-1}$, △: $[Ti^{II}OPc^{-2}]^{-2}$, ▽: $[Ti^{II}OPc^{-3}]^{-3}$, ☆: $[Ti^{IV}OPc^{-2}]^{+1}$.

306 nm increase slightly in intensity. These spectral changes are similar with the spectral changes of ring-based reduction process of MPc having redox inactive metal centers [26–31]. Thus, we can assign this process to a ring-based reduction, $[Cl–Ga^{III}Pc^{-2}]/[Cl–Ga^{III}Pc^{-3}]^{1-}$. The only difference is the band at 634 nm. While the Q band decreases in intensity without shift, a new band is recorded between 500 and 600 nm during the first reduction process of MPc having redox inactive metal centers [33–38]. These changes are also recorded with GaPc; however, an extra band is recorded at 634 nm. We have observed well-defined isosbestic points at 638 and 783 nm. These isosbestic points demonstrate that the reduction proceeds cleanly in deoxygenated DCM to give a single, reduced species. Further reduction of the complex under applied potential at −1.40 V indicated the $[Cl–Ga^{III}Pc^{-3}]^{1-}/[Cl–Ga^{III}Pc^{-4}]^{2-}$ process. During the first oxidation of the complex, the Q band decreases without shift and two new bands increase at 512 and 871 nm [figure 8(b)],

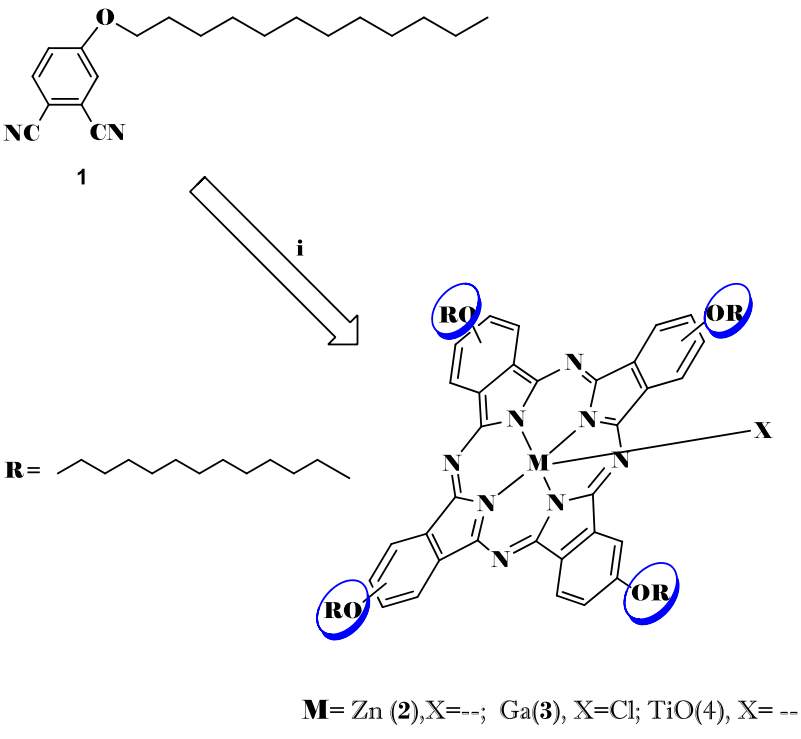

Scheme 1. Synthetic route of 2(3), 9(10), 16(17), 23(24)-tetrakis undecyloxy phthalocyanine M{Pc[O-$(CH_2)_{11}CH_3$)]$_4$} (M = Zn(**2**), Ga(**3**), Ti(**4**)).

which indicates a ring-based oxidation process. During the second oxidation reaction, spectral changes indicated decomposition of the complex at the end of the oxidation process. The color change of the solution of the complexes during the redox processes was recorded using *in situ* colorimetric measurements without any potential application. The solution of [Cl–$Ga^{III}Pc^{-2}$] is bluish green ($x = 0.311$ and $y = 0.3809$) [figure 8(c)]. As the potential is stepped from 0 to −1.00 V, color of the neutral [Cl–$Ga^{III}Pc^{-2}$] changes and light blue color ($x = 0.2796$ and $y = 0.3165$) for monoanionic form of [Cl–$Ga^{III}Pc^{-3}]^{1-}$ was obtained at the end of the first reduction. During the oxidation process, color of the complex is slightly decreased and a light green color ($x = 0.3352$ and $y = 0.3761$) is recorded for the monocationic species, [Cl–$Ga^{III}Pc^{-1}]^{1+}$.

Figure 9 shows *in situ* UV–vis spectral changes of the neutral and electro-generated species during the reduction/oxidation processes of [$Ti^{IV}OPc^{-2}$] (**4**). During the controlled potential reduction of **4** at −0.75 V [figure 9(a)], while the absorption of the Q band corresponding to the neutral [$Ti^{IV}OPc^{-2}$] species decreases without shift, a new band is recorded at 594 nm. At the same time, a new band corresponding to the electro-generated species appears at 950 nm. As shown in figure 9(a), the process occurred with clear isosbestic points at 411, 454, 636, and 766 nm in the spectra which demonstrate that there is no chemical reaction complicating the electron transfer reaction. These spectral changes are typical for a metal-based reduction of titanyl phthalocyanine complexes [37, 39–41]. During the controlled potential reduction of **4** at −1.25 V, the absorption for the Q band at 594 nm

shifts to 586 nm with decreasing intensity, while a new band is recorded at 553 nm. During this potential application, the bands at 965 nm decrease in intensity, while a new band is recorded at 915 nm. These spectral changes are easily assigned to the $[Ti^{III}OPc^{-2}]^{-1}/[Ti^{II}OPc^{-2}]^{-2}$ redox process [figure 9(b)] [37, 39–41]. This process has isosbestic points at 444, 580, and 803 nm in the spectra. During further reduction of the complex at −1.75 V, spectral changes indicate a Pc-based reduction process [figure 9(b) inset]. The spectral changes given in figure 9(c) indicate Pc ring reduction under the applied potential at −1.90 V. Complex **4** oxidized to $[Ti^{IV}OPc^{-1}]^{1+}$ and then decomposes under the applied potential at 0.80 V, because while the Q band decreases in intensity without shift, new bands increase at 535 and 877 nm. However, these new bands could not increase due to decomposition of the oxidized species [figure 9(c)]. Color changes of **4** in solution during the redox processes were recorded with *in situ* electrocolorimetric measurements and are given in figure 9(d).

4. Conclusion

The synthesis of new soluble metallophthalocyanine complexes [Zn(II), Ga(III), and Ti(IV)] **2–4** was characterized by FT-IR, ^{1}HNMR, ^{13}CNMR, UV–vis, and MALDI-MS spectra, and also surface morphologies were determined by AFM. Voltammetric and spectroelectrochemical studies indicate that while zinc and gallium phthalocyanines have only ring-based, multi-electron, redox processes, titanium phthalocyanine gives both metal and ring-based reduction processes. Definite determination of the colors of the electrogenerated anionic and cationic forms of the complexes with chromaticity measurements is important to decide the possible electrochromic application of the complexes. Different color of the electrogenerated species indicates their possible application in display technologies, e.g. electrochromic and data storage applications.

Acknowledgements

We thank the research fund of Sakarya University and TUBİTAK (Project No: BAP-2013-02-04-049, Project No: TBAG-108T094).

References

[1] F.I. Bohrer, C.N. Colesniuc, J. Park, I.K. Schuller, A.C. Kummel, W.C. Trogler. *J. Am. Chem. Soc.*, **130**, 3712 (2008).
[2] B.A. Minch, W. Xia, C.L. Donley, R.M. Hernandez, C. Carter, M.D. Carducci, A. Dawson, D.F. O'Brien, N.R. Armstrong. *Chem. Mater.*, **17**, 1618 (2005).
[3] M. Kimura, T. Muto, H. Takimoto, K. Wada, K. Ohta, K. Hanabusa, H. Shirai, N. Kobayashi. *Langmuir*, **16**, 2078 (2000).
[4] M.N. Sibata, A.C. Tedesco, J.M. Marchetti. *Eur. J. Pharm. Sci.*, **23**, 131 (2004).
[5] K. Ishii, M. Shiine, Y. Shimizu, S. Hoshino, H. Abe, K. Sogawa, N. Kobayashi. *J. Phys. Chem. B*, **112**, 3138 (2008).
[6] H.S. Majumdar, A. Bandyopadhyay, A.J. Pal. *Org. Electron.*, **4**, 39 (2003).
[7] D. Dini, M. Hanack, H.-J. Egelhaaf, J.C. Sancho-Garcia, J. Cornil. *J. Phys. Chem. B*, **109**, 5425 (2005).
[8] A.D. Dinsmore, M.F. Hsu, M.G. Nikolaides, M. Marquez, A.R. Bausch, D.A. Weitz. *Science*, **298**, 1006 (2002).

[9] M.F. Craciun, S. Rogge, A.F. Morpurgo. *J. Am. Chem. Soc.*, **127**, 12210 (2005).
[10] C.C. Leznoff, A.B.P. Lever. In *Phthalocyanines: Properties and Applications*, C.C. Leznoff, A.B.P. Lever (Eds), Vol. 1–4, pp. 86–90, VCH, Weinheim (1989–1996).
[11] M.N. Yaraşir, M. Kandaz, A. Koca, B. Salih. *Polyhedron*, **26**, 1139 (2007).
[12] L.A. Ehrlich, P.J. Skrdla, W.K. Jarrell, J.W. Sibert, N.R. Armstrong, S.S. Saavedra, A.G.M. Barrett, B.M. Hoffman. *Inorg. Chem.*, **39**, 3963 (2000).
[13] S.L.J. Michel, A.G.M. Barrett, B.M. Hoffman. *Inorg. Chem.*, **42**, 814 (2003).
[14] M.N. Yaraşır, M. Kandaz, A. Koca, B. Salih. *J. Porphyrins Phthalocyanines*, **10**, 1022 (2006).
[15] M.N. Yarasır, M. Kandaz, B.F. Filiz Şenkal, A. Koca, B. Salıh. *Dyes Pigm.*, **77**, 7 (2008).
[16] P. Tau, T. Nyokong. *Polyhedron*, **25**, 1802 (2006).
[17] M. Kandaz, Ö. Bekarolu. *Chem. Ber.*, **130**, 1833 (1997).
[18] J.H. Brannon, D. Magde. *J. Am. Chem. Soc.*, **102**, 62 (1980).
[19] A. Ogunsipe, T. Nyokong. *J. Photochem. Photobiol. A: Chem.*, **173**, 211 (2005).
[20] I. Seotsanyana-Mokhosi, N. Kuznetsova, T. Nyokong. *J. Photochem. Photobiol. A: Chem.*, **140**, 215 (2001).
[21] J. Simon, P. Bossoul. In , *Phthalocyanines: Properties and Applications*, C.C. Leznoff, A.B.P. Lever (Eds), Vol. 2, pp. 223–225, VCH, New York (1993).
[22] M. Ozcesmeci, I. Ozcesmeci, E. Hamuryudan. *Polyhedron*, **29**, 271 (2010).
[23] N.S. Bayliss. *J. Chem. Phys.*, **18**, 292 (1950).
[24] W.F. Law, R.C.W. Liu, J.H. Jiang, D.K.P. Ng. *Inorg. Chim. Acta*, **256**, 147 (1997).
[25] S. Maree, T. Nyokong. *J. Porphyrins Phthalocyanines*, **5**, 782 (2001).
[26] A.B.P. Lever, P.C. Minor, J.P. Wilshire. *Inorg. Chem.*, **20**, 2550 (1981).
[27] B. Akkurt, A. Koca, E. Hamuryudan. *New J. Chem.*, **33**, 2248 (2009).
[28] Ö.A. Osmanbaş, A. Koca, İ. Özçeşmeci, Aİ. Okur, A. Gül. *Electrochim. Acta*, **53**, 4969 (2008).
[29] A. Koca, M. Özçeşmeci, E. Hamuryudan. *Electroanalysis*, **22**, 1623 (2010).
[30] M. Özer, A. Altındal, A.R. Özkaya, M. Bulut, Ö. Bekaroğlu. *Polyhedron*, **25**, 3593 (2006).
[31] A.B.P. Lever, E.R. Milaeva, G. Speier. In *Phthalocyanines: Properties and Applications*, C.C. Leznoff and A.B.P. Lever (Eds), Vol 3, pp. 5–27. VCH, New York (1993).
[32] P.T. Kissinger, W.R. Heineman. *Laboratory Techniques in Electroanalytical Chemistry*, 2nd Edn, pp. 51–163, Marcel Dekker, New York (1996).
[33] L.D. Rollmann, R.T. Iwamoto. *J. Am. Chem. Soc.*, **90**, 1455 (1968).
[34] D. Kulaç, M. Bulut, A. Altındal, A.R. Özkaya, B. Salih, Ö. Bekaroğlu. *Polyhedron*, **26**, 5432 (2007).
[35] A. Koca, Ş. Bayar, H.A. Dinçer, E. Gonca. *Electrochim. Acta*, **54**, 2684 (2009).
[36] N. Nombona, T. Nyokong. *Dyes Pigm.*, **80**, 130 (2009).
[37] G. Mbambisa, P. Tau, E. Antunes, T. Nyokong. *Polyhedron*, **26**, 5355 (2007).
[38] A. Alemdar, A.R. Özkaya, M. Bulut. *Polyhedron*, **28**, 3788 (2009).
[39] A. Koca, A.R. Özkaya, Y. Arslanoğlu, E. Hamuryudan. *Electrochim. Acta*, **52**, 3216 (2007).
[40] P. Tau, T. Nyokong. *Dalton Trans.*, 4482 (2006).
[41] P. Tau, T. Nyokong. *Polyhedron*, **25**, 1802 (2006).